Finite Element Analysis of UHPC Corbels

Hussein Al-Quraishi
Lecturer
Building and Construction Engineering Department, University of Technology
Hussain.abbas@yahoo.com

Ahmed Fuad
Lecture
Building and Construction Engineering Department, University of Technology
Ahmed_Fuaq@yahoo.com

ABSTRACT

Finite element method is the most widely numerical technique used in engineering field. Through the study of behavior of concrete material properties, various concrete constitutive laws and failure criteria have been developed to model the behavior of concrete. A feature of the Finite Element program (ATENA) is used in this study to model the behavior of UHPC corbel under concentrated load only. The Finite Element (FE) model is followed by verification against experimental results. Some variable effects on the shear capacity of the UHPC corbels are also demonstrated in a parametric study.

A proposed design equation of shear strength of UHPC corbel was presented and checked with numerical results.

Keywords: Ultra high performance concrete, corbel, numerical analysis, design equation.

التحليل بطريقة العناصر المحددة للكتائف الخرسانية عالية الكفاءة

حسين القريشي
مدرس
قسم هندسة البناء والانشاءات-الجامعة التكنولوجية

احمد فؤاد
مدرس
قسم هندسة البناء والانشاءات-الجامعة التكنولوجية

الخلاصة

طريقة العناصر المحددة من الطرق العددية الواسعة الانتشار في مجال الهندسة. من خلال دراسة تصرف خواص الخرسانة مختلف القوانين الحاكمة للفشل قد طورت لنمذجة تصرف الخرسانة. برنامج خاص للعناصر المحددة استخدم لدراسة تصرف الكتائف المصنوع من مادة الخرسانة العالية الكفاءة وتحت تأثير قوة مركزة فقط. نتائج موديل العناصر المحددة قد قورن بالفحوصات العملية المنفذة سابقا. بعض المتغيرات المؤثرة على مقاومة القص للكتائف المصنوعة من الخرسانة عالية الكفاءة تم دراستها. مقترح معادلة تصميمية لمقاومة القص للكتائف الخرسانية عالية الكفاءة تم عرضه ومقارنته مع نتائج التحليل العددي.

الكلمات الرئيسية: خرسانة ذات كفاءة عالية، عضو الساند،تحليل عددي، معادلة تصميمية.

1. INTRODUCTION

Ultra-high-performance concrete (UHPC) is a new type of concrete that is being developed by agencies concerned with infrastructure protection. UHPC is characterized by being a steel fiber-reinforced cement composite material with compressive strengths in excess of 150 MPa, up to and possibly exceeding 250 MPa. UHPC is also characterized by its constituent material make-up: typically fine-grained sand, silica fume, small steel fibers, and special blends of high-strength Portland cement. Note that there is no coarse aggregate. The production types of UHPC used in constructing the UHPC corbels are produced by Kassel University/ Germany namely M3Q has a compressive strength around 200 MPa and a tensile strength ranges from 4 to 12 MPa depending on fiber content.

Corbels are structural members very commonly used in reinforced concrete structures and particularly in precast structures where their principal function is the transfer of the vertical and horizontal forces to principal members.

Corbels are structural members characterized by shear span-depth ratio (a/d) generally less than unity and subjected to concentrated forces as in the support zones.
The main objective of this study is:

- Present a numerical model for UHPC corbels subjected to concentrated force using finite element analysis for further parametric study.
- Highlighting the role of the parameters that influence the performance of UHPC corbels including geometric dimensions effect, influence of reinforcement ratio, influence of tensile strength, and shear span-depth ratio effect.
- Present design equation for predicting the shear strength of UHPC corbel.

2. FINITE ELEMENTS ANALYSIS

Finite element analysis is a numerical technique used by engineers to find solution for different problems. Fundamental assumption of the method states, that the domain can be divided into smaller regions in which the equations can be solved. By assembling the solution for each region, the behavior of all structure can be described. The region can be divided into finite number of elements and these elements connected by nodes.
ATENA software program were used for the numerical modeling in this study, **Cervenka, 2009**. In ATENA, 3D isoparametric element with 20 nodes was used to represent the cantilevered concrete of corbels, as shown in **Fig. 1**. Also, the same nodes were used to model the column which contact with the cantilevered corbels. Each node has three degrees of freedom.

3. MATERAL MODELING

The material model takes into consideration the UHPC strain softening after both cracking and crushing. The experimental test results of cylinders, prisms and reinforcement bars taken from **Al-Quraishi, 2014** were used in the Finite Element Analysis (FEA).
The results of Finite element analysis largely depend on material model and exterior boundary conditions. Compression behavior in hardening and softening, fracture of concrete in tension based on nonlinear fracture mechanics, compressive strength reduction after tension cracking, tension stress deterioration due to compression cracking, shear retention factor, crack models and modeling of tension reinforcement were included in the material models.
Only a half of the corbel was symmetrically modeled for numerical analysis. Due to nonlinear material behavior, redistribution of internal forces was taken into account after each displacement increment to satisfy deformations compatibility and forces equilibrium.
In ATENA, the material model **CC3NonLinCementitious2User** was chosen to simulate the UHPC, allowing user to define new laws for the material behavior. This model consists of combined fracture-plastic constitutive model. Rankine failure criterion with a fixed crack model was used to simulate the tension behavior of concrete. The Menétrey-Willam failure surface was used to model the compression behavior of concrete. In Menétrey-Willam, the position of failure surface is not fixed, but can be moved along the hydrostatic axis simulating hardening and softening stages, **Cervenka, 2009**.
The test results of direct tensile test of prisms taken from **Al-Quraishi, 2014** are used in the numerical analysis to simulate the tensile-displacement behavior in tension. The displacement was normalized with the characteristics length which is equal to the projection length of finite element mesh according to ATENA to get the stress-strain relationship, as shown in **Fig. 2**.
The shear stiffness or shear modulus of concrete reduced after cracking. Across the cracks, the dowel action of steel bars contributes to the shear stiffness. The factors affecting shear stiffness are crack width and reinforcement ratio, whereas to include these effects, appropriate value of shear

modulus (G) must be used. Appropriate shear stiffness softening after cracking for UHPC according to **Fehling and Ismail, 2012** was used in this study, as shown in **Fig. 3**.
The experimental compressive strength of cylinder from **Al-Quraishi, 2014** was adopted in the material model to simulate the compression behavior after converting the stress-displacement relationship to stress-strain relationship by dividing the displacement over characteristics length which is equal to 20cm (length of concrete cylinder), as shown in **Fig. 4**.
In the case of corbel under concentrated load, a realistic modeling of reinforced concrete needs to consider a corbel subjected to multiaxial stress state, not uniaxial. The compressive strength of concrete can substantially decrease in relation to the compressive strength of cylinder by the transverse of tension cracking. The reduction of compressive strength of UHPC after tension cracking is done in similar way as in **Fehling et al., 2008**, as shown in **Fig. 5**.
The tensile strength of concrete can also substantially decrease in relation to uniaxial tensile strength by increasing transverse compressive stress in relation to compressive stress of cylinder according to work of **Jürgen et al., 2008**, as shown in **Fig. 6**.
The steel reinforcement is modeled by bilinear stress-strain relationship with hardening as shown in **Fig. 7**.
In FEA of reinforced concrete structures, two approaches have been employed for crack modeling namely discrete cracks at element nodes and smeared crack within the element with fixed or variable directions, a smeared crack model was adopted. The load was increased by deformation control in steps with the iterative solver of standard Newton-Raphson method.

4. GEOMETRIC MODELING OF CORBEL

The corbels taken from **Al-Quraishi 2015** were simply supported along two edges and subjected to concentrated load at the center of the column. **Fig. 8** shows the overall dimensions of tested corbels.
Table 1 shows the properties of the tested UHPC corbels C1-ρ1.2 and C2-Ref by **Al-Quraishi, 2015** in which, the first column represents the name of the corbel, $f_c^{'}$ represents the compressive strength of concrete, f_{te} means tensile strength of concrete, a/d means shear span to depth ratio, d_{bar} is the diameter of tension reinforcement bar, ρ is the reinforcement ratio, f_y is the yield stress of tension reinforcement
Due to symmetry, a half of the corbel was modeled for simplification in FEA. The load was applied on the corbel by a deformation control through steel plate with a deformation step of 7E-05 m.
The corbel zone was discretized with tetrahedral element within the cantilevering area. The same discretized were used in the column area; **Fig. 9** represents the model geometry used.
Due to the boundary conditions of the experimental tests, edges of the corbels are free to lift upwards. Spring surface elements with stiffness zero in tension and actual test setup stiffness in compression were used under the steel plate.

5. NUMERICAL ANALYSIS OF C2-Ref AND C1-ρ1.2 CORBEL

To verify the validity and accuracy of the adopted numerical model (geometrical and material model), and to check the ability of the constitutive model to simulate the behavior of UHPC corbel under vertical load only; the numerical result was compared with the experimental result for the reference corbel C2-Ref (corbel with 0.48% reinforcement ratio) and C1- ρ1.2 (corbel with 1.2% reinforcement ratio) tested by the **Al-Quraishi, 2015**. Through the ultimate shear capacity, the ratio of numerical to the experimental result is 0.94 and 1.02 for C2-Ref and C1- ρ1.2 corbel respectively, which shows a good prediction of adopted model. From **Fig. 10** and **11**, the stiffness of experimental load-deflection curved is higher than the numerical load-deflection curve. Also, the numerical

results show more nonlinear behavior before the maximum load in comparison with the experimental results.

6. PARAMETRIC ANALYSIS

A very good prediction of numerical model to the shear strength capacity of UHPC corbel leads to study the factors effect on corbel shear strength through a parametric analysis. This parametric analysis helps to get more tests results that could not make it at the lab due to high cost of UHPC material. The properties of UHPC corbel (C2-Ref) is used as the reference in this parametric analysis.

6.1 Influence of Tensile Strength of Concrete

The tensile strength of UHPC corbel depends mainly on the steel fiber content. The specimen C2-Ref was taken as reference to study the influence of tensile strength (f_t) on UHPC corbel shear strength. By keeping other variables constant, decrease the tensile strength from 3.9 (0.5% steel fiber content) to 1 MPa (0.1% steel fiber content), the shear strength was decrease from 303 kN to 148.8 kN. While, when the tensile strength increases from 3.9 (0.5% steel fiber content) to 14 MPa (2.5% steel fiber content), the shear strength increases from 303 kN to 616 kN (see **Table 2**). **Fig. 12** shows the load-deflection curve for different tensile strength of concrete. Also, shear strength of corbel increases with tensile strength as the 0.54 power function (see **Fig. 13**). The increase of shear strength of the corbel due to tensile strength increase was expectedly, because concrete shear strength of corbel represented by tensile resistance along the critical section.

6.2 Shear Span-Depth Ratio

Shear span-depth ratio is very important factor on shear strength of corbel, by which the corbel failure transferred from flexural to shear when the shear span-depth ratio decreased. As already pointed, the reference corbel C2-Ref has shear span-depth ratio (a/d) equal to 0.5, by increase the a/d ratio to 0.9, the shear capacity decreased from 303 kN to 142 kN. While, by decreasing the a/d ratio to 0.1, the corbel shear capacity increase from 303 kN to 1303 kN (see **Table 2**). **Fig. 14** shows the load-deflection curve for different shear span-depth ratio. **Fig. 15** shows shear strength of the corbel decreases with the power function of 0.98 with shear span-depth ratio increased.

6.3 Influence of Reinforcement Ratio

The influence of tension reinforcement ratio on shear strength of corbels had been studied by increasing the reinforcement ratio of C2-Ref corbel from 0.47% to 2.5%. By increasing the reinforcement ratio from 0.47% to 2.5%, the shear strength increased from 303 kN to 1038 kN (see **Table 1**). The load-deflection curve for different reinforcement ratio is shown in **Fig. 16**. It is shown in **Fig. 17** that the shear strength of the corbels has approximately 0.74 power functions with reinforcement ratio increased.

6.4 Geometric Dimensions Effect

The shear capacity of corbel not only depends on properties of the material but also depends on geometrical dimension of the corbels, i.e. the depth and width of the corbel. The reference corbel (C2-Ref) has a width of 150 mm and depth of 250 mm (b.d=33000). To study this effect a new geometrical dimension of corbels were tested using ATEN. The width of the corbel ranged from 50 mm to 250mm and effective depth ranged from 120 mm to 320 mm. Decreasing the width and depth of the corbel to 50mm and 120mm respectively, decreases the shear strength of the corbel to 86.6

kN. While, increasing the width and depth to 250mm and 320 mm respectively, increases the shear strength of corbel to 589.3 kN (see **Table 2**). **Fig. 18** shows the load-deflection curve for different dimensions b and d. **Fig.19** shows the behavior influence function of geometric dimensions on the shear capacity of the UHPC corbel.

7. PROPOSED DESIGN EQUATION

The ultimate load capacity of the corbel depends on properties of the material, geometry of the corbel and position of the applied vertical load from the support. Furthermore, the presence of a horizontal load also has significant effect on the corbel's vertical load carrying capacity. The best fit expression for estimating the load-carrying capacities of corbels (without stirrups) subjected to vertical load only, which was based on a statistical analysis of numerical results is presented here.
The general form of expression has the following form:

$$V=K1\,(b.d)^{K2}\,(f_t)^{K3}\,(a/d)^{K4}\,(As/b.d)^{K5} \quad \ldots\ldots(1)$$

Where:
V is the nominal shear capacity of the corbel, K_1 through K_5 are constant, b. d are the corbel width and effective depth, f_t is the tensile strength of concrete, a/d is the shear span-depth ratio, and As is the area of tension reinforcement.
The coefficient K1=0.44 is obtained from regression analysis. K2=0.74, K3=0.54, K4=0.98, and K5=0.74 are obtained from influence function of each factor in parametric analysis.
So, the final form of the corbel shear capacity is:

$$V=0.44\,[(b.d)^{0.74}\,(136/(a/d)^{0.98})\,(f_t)^{0.54}\,(As/b.d)^{0.74}] \quad \ldots\ldots(2)$$

From **Fig. 20** and **Table 2**, comparison between the numerical shear strength of UHPC corbel (from ATENA) and proposal shear strength of corbel (from **Equation 2**), shows the two sets of values are in satisfactory agreement. The standard deviation for ($V_{numerical}$ / $V_{proposal}$) is 0.05 and R^2=0.98.

8. CONCLUSIONS

Through the material and geometrical finite element modeling of UHPC corbel, some of factors affecting the shear strength of UHPC corbels were presented in parametric study to propose design equation of shear strength of UHPC corbel under concentrated load. The proposed design equation shows good prediction for shear strength of UHPC corbel in comparison with the 66 numerical results presented in this study. This equation is shown to be applicable for a wide range of parametric variations; ranging between 1 MPa to 14 MPa in tensile strength of UHPC, from 0.1% to 2.5% steel fiber content, from 0.1 to 0.9 in shear span-depth ratio, from 0.47 to 2.5 in reinforcement ratio and from 6000 to 80000 in geometric dimensions (b.d).

REFERENCES

- Al-Quraishi H., 2014, *Punching shear behavior of UHPC Flat slabs*, Ph.d Thesis, University of Kassel/Germany.

- Al-Quraishi H., 2015, *Behavior of UHPC corbels: reinforcement ratio effect*, The 2nd International Conference of Buildings, Construction and Environmental Engineering Department-Beirut (BCEE2-2015).

- Cervenka Consulting, 2009, *ATENA program documentation*, Prague, Czech Republic.

- Fehling E., and Ismail M., 2012, *Expermintelle und numerische untersuchungen von betwehrten UHPC-bauteilen unter reiner torsion*, Deutscher Ausschuss für Stahlbeton.

- Fehling E., Leutbecher T., Röder F., Stürwald S., 2008, *Structural behavior of UHPC under biaxial loading*, Second International Symposium on Ultra High Performance Concrete.

- Fehling E., Leutbecher T., Friedrich R. and Simomne S., 2008, *Structural behavior of UHPC under biaxial loading*, Second International Symposium on Ultra High Performance Concrete-Germany.

- Fattuhi N., 1994, *Reinforced corbels made with plain and fibrous concretes*; ACI Structural Journal.

- Fattuhi N., 1986, *SFRC corbel tests*, ACI Structural Journal.

- Jürgen G., Ludger L., Christian E. and Maik W., 2008, *Multi-axial and Fatiguue behavior of ultra-high-performance concrete (UHPC)*, Second International Symposium on Ultra High Performance Concrete-Germany.

- Kolmar W., 1985, *Beschreibung der Kraftubertragunguber Risse in nichtlinearen Finite ElementBerechnungen von Stahlbetontragwerken*, Thesis, TU Darmstadt, Darmstadt-Germany.

- Yong Y. and Balaguru P., 1994, *Behavior of reinforced high strength concrete corbels*, Journal of Structural Engineering.

Table 1: Characteristics of tested corbels from reference [6]

Corbel	Concr-ete type	f_c' (MPa)	f_{te} (MPa)	a/d	fiber content (%)	E (MPa)	d_{bar} (mm)	ρ (%)	f_y (MPa)
C1-ρ1.2	UHPC	198.5	4.0	0.5	0.5	49024	10.5	1.2	560
C2-Ref	UHPC	198.9	3.9	0.5	0.5	49050	10.5	0.48	560

Table 2: Numerical and proposal shear loads of UHPC corbel

No.of Corbel	f_t (MPa)	a/d	b.d (mm^2)	reinf.ratio (%)	$f_{c'}$ (MPa)	$V_{numerical}$ (kN)	$V_{proposal}$ (kN)	$V_{proposal}/V_{numerical}$
1	1	0.5	33000	0.47	198.5	148.80	148.95	1.00
2	2	0.5	33000	0.47	198.5	214.57	216.57	1.00
3	3	0.5	33000	0.47	198.5	266.88	269.58	1.01
4	3.9	0.5	33000	0.47	198.5	310.20	310.62	1.00
5	4	0.5	33000	0.47	198.5	311.56	314.89	1.01

6	5	0.5	33000	0.47	198.5	351.31	355.22	1.01
7	6	0.5	33000	0.47	198.5	387.53	391.97	1.01
8	7	0.5	33000	0.47	198.5	421.04	425.99	1.01
9	8	0.5	33000	0.47	198.5	452.41	457.84	1.01
10	9	0.5	33000	0.47	198.5	482.01	487.91	1.01
11	10	0.5	33000	0.47	198.5	510.13	516.48	1.01
12	11	0.5	33000	0.47	198.5	536.98	543.75	1.01
13	12	0.5	33000	0.47	198.5	562.72	569.91	1.01
14	13	0.5	33000	0.47	198.5	587.48	595.09	1.01
15	14	0.5	33000	0.47	198.5	616.20	619.38	1.00
16	3.9	0.1	33000	0.47	198.5	1303.31	1503.90	1.15
17	3.9	0.2	33000	0.47	198.5	660.29	762.44	1.15
18	3.9	0.3	33000	0.47	198.5	443.6	512.43	1.15
19	3.9	0.4	33000	0.47	198.5	334.52	386.54	1.15
20	3.9	0.5	33000	0.47	198.5	268.75	310.61	1.15
21	3.9	0.6	33000	0.47	198.5	224.74	259.79	1.15
22	3.9	0.7	33000	0.47	198.5	193.2	223.36	1.15
23	3.9	0.8	33000	0.47	198.5	169.47	195.97	1.15
24	3.9	0.9	33000	0.47	198.5	150.98	174.60	1.15
25	3.9	0.5	6000	0.47	198.5	86.67	87.97	1.01
26	3.9	0.5	7800	0.47	198.5	105.25	106.82	1.01
27	3.9	0.5	9800	0.47	198.5	124.61	126.48	1.01
28	3.9	0.5	12000	0.47	198.5	144.76	146.93	1.01
29	3.9	0.5	14400	0.47	198.5	165.67	168.15	1.01
30	3.9	0.5	17000	0.47	198.5	187.33	190.13	1.01
31	3.9	0.5	19800	0.47	198.5	209.7	212.84	1.01
32	3.9	0.5	22800	0.47	198.5	232.78	236.26	1.01
33	3.9	0.5	26000	0.47	198.5	256.54	260.38	1.01
34	3.9	0.5	29400	0.47	198.5	280.96	285.17	1.01
35	3.9	0.5	33000	0.47	198.5	306.03	310.61	1.01
36	3.9	0.5	36800	0.47	198.5	331.74	336.70	1.01
37	3.9	0.5	40800	0.47	198.5	358.06	363.42	1.01
38	3.9	0.5	45000	0.47	198.5	384.99	390.75	1.01
No.of Corbel	f_t (MPa)	a/d	b.d (mm^2)	reinf.ratio (%)	$f_{c'}$ (MPa)	$V_{numerical}$ (kN)	$V_{proposal}$ (kN)	$V_{proposal}/V_{numerical}$
39	3.9	0.5	49400	0.47	198.5	412.5	418.68	1.01
40	3.9	0.5	54000	0.47	198.5	440.6	447.19	1.01
41	3.9	0.5	58800	0.47	198.5	469.26	476.28	1.01
42	3.9	0.5	63800	0.47	198.5	498.47	505.93	1.01
43	3.9	0.5	69000	0.47	198.5	528.23	536.13	1.01
44	3.9	0.5	74400	0.47	198.5	558.52	566.88	1.01
45	3.9	0.5	80000	0.47	198.5	589.33	598.15	1.01
46	3.9	0.5	33000	0.47	198.5	303.2	310.61	1.02
47	3.9	0.5	33000	0.6	198.5	372.35	372.14	0.99
48	3.9	0.5	33000	0.7	198.5	417.4	417.10	0.99
49	3.9	0.5	33000	0.8	198.5	460.8	460.42	0.99

50	3.9	0.5	33000	0.9	198.5	502.82	502.36	0.99
51	3.9	0.5	33000	1	198.5	543.65	543.09	0.99
52	3.9	0.5	33000	1.1	198.5	583.42	582.78	0.99
53	3.9	0.5	33000	1.2	198.5	659.1	621.54	0.94
54	3.9	0.5	33000	1.3	198.5	660.29	659.46	0.99
55	3.9	0.5	33000	1.4	198.5	697.56	696.64	0.99
56	3.9	0.5	33000	1.5	198.5	734.15	733.13	0.99
57	3.9	0.5	33000	1.6	198.5	770.1	768.99	0.99
58	3.9	0.5	33000	1.7	198.5	805.48	804.28	0.99
59	3.9	0.5	33000	1.8	198.5	840.33	839.03	0.99
60	3.9	0.5	33000	1.9	198.5	874.67	873.28	0.99
61	3.9	0.5	33000	2	198.5	908.55	907.06	0.99
62	3.9	0.5	33000	2.1	198.5	942.1	940.41	0.99
63	3.9	0.5	33000	2.2	198.5	975.03	973.34	0.99
64	3.9	0.5	33000	2.3	198.5	1007.68	1005.89	0.99
65	3.9	0.5	33000	2.4	198.5	1039.96	1038.08	0.99
66	3.9	0.5	33000	2.5	198.5	1038.1	1069.92	1.03

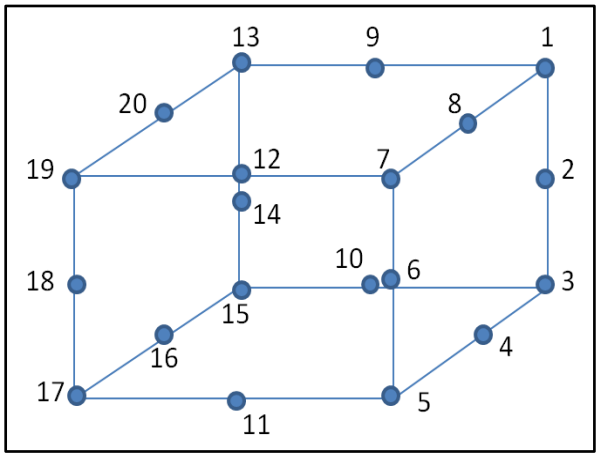

Figure 1. 20 nodes solid isoparametric elements.

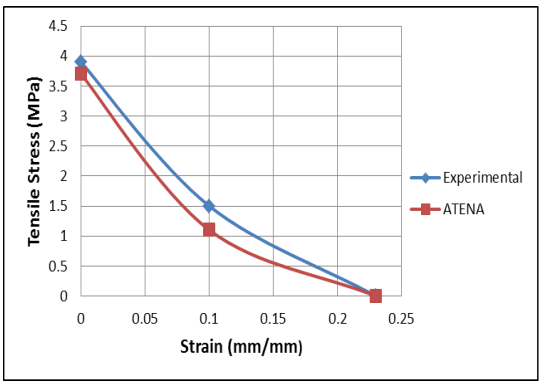

Figure 2. ATENA and experimental tensile stress-strain curve

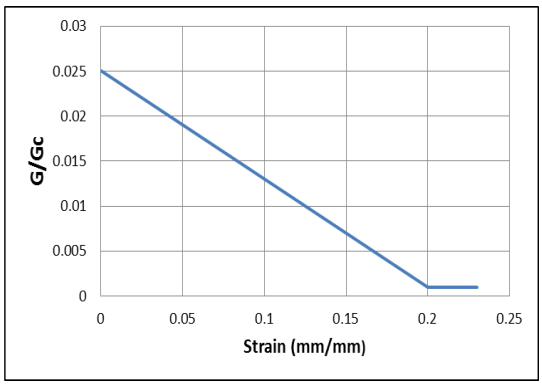

Figure 3. Shear retention factor

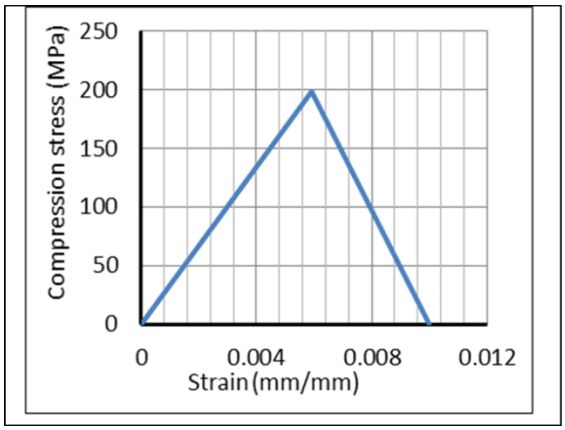

Figure 4. Compression behavior of UHPC

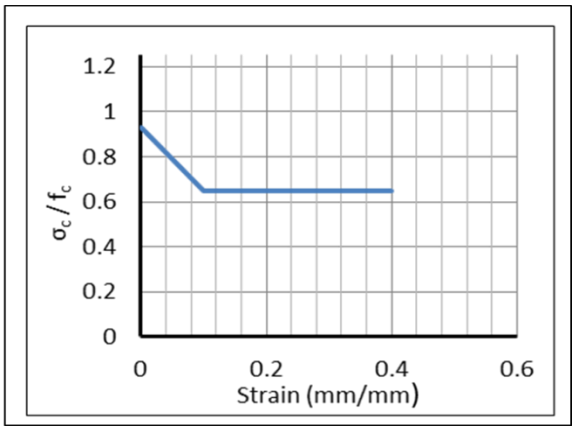

Figure 5. Strength reduction in compression of UHPC due to tension cracking

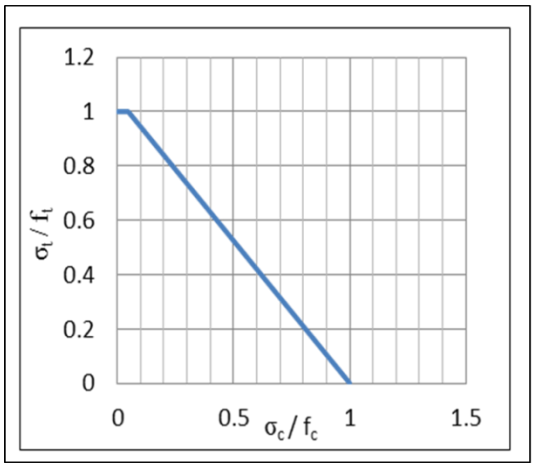

Figure 6. Tensile stress deterioration due to transverse compressive stress

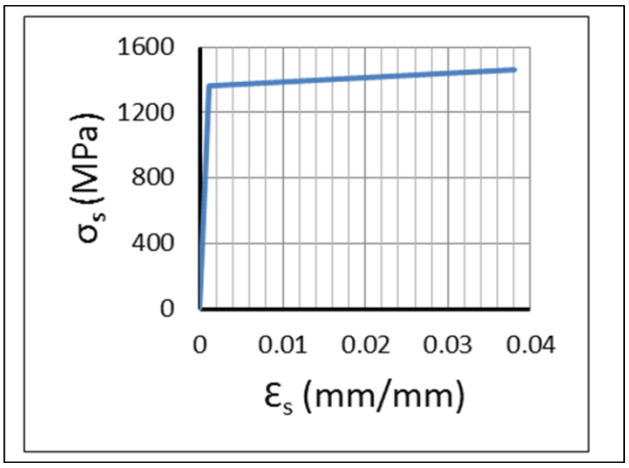

Figure 7. Bilinear behavior with hardening stress-strain law for reinforcement

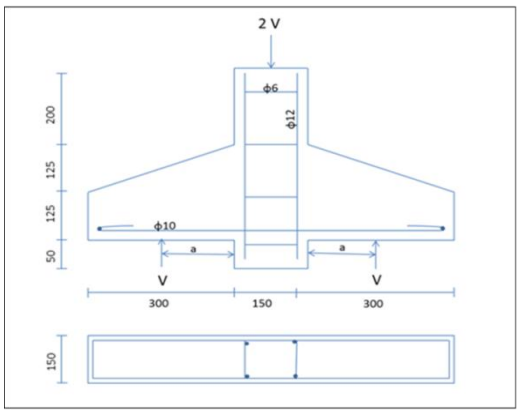

Figure 8. Overall dimensions of corbels

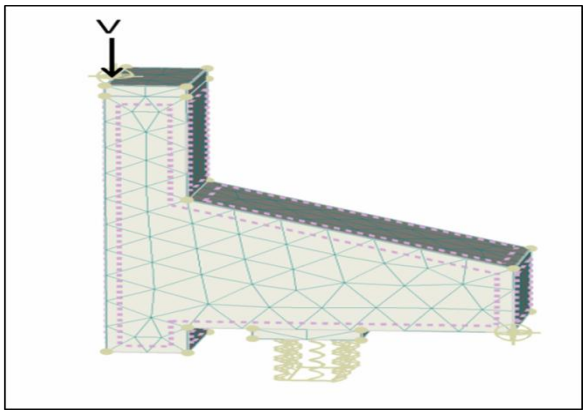

Figure 9. Three dimensional corbel model in ATENA

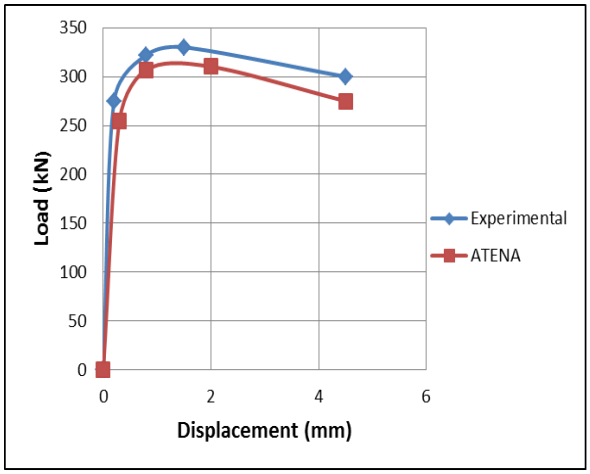

Figure 10. Load-displacement curve of C2-Ref corbel

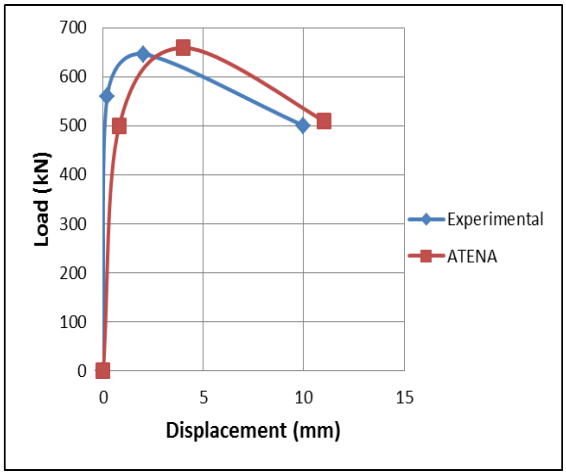

Figure 11. Load-displacement curve of C1-ρ1.2 corbel

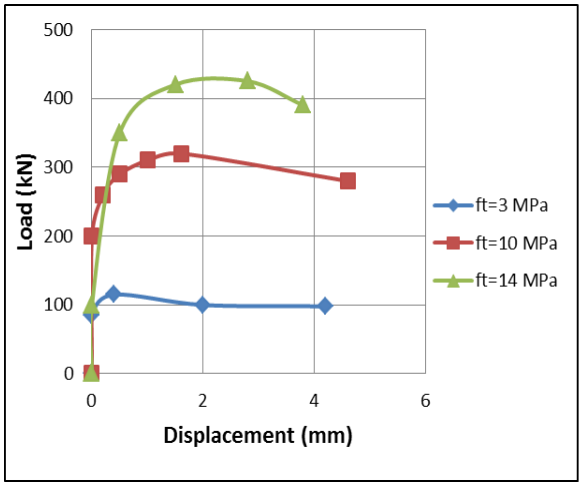

Figure 12.Load-deflection curve for different tensile strength of concrete

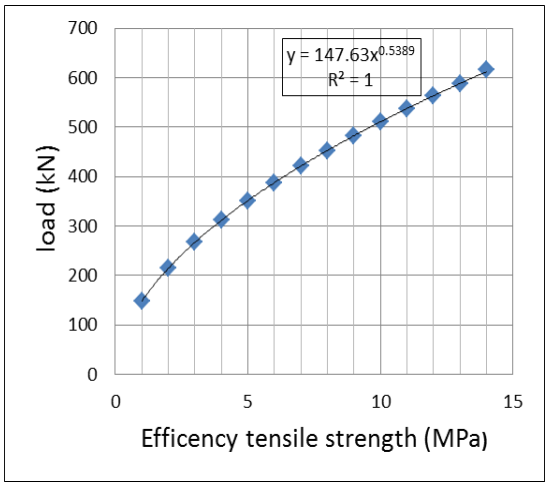

Figure 13. Influence function of tensile strength on shear strength of UHPC corbel

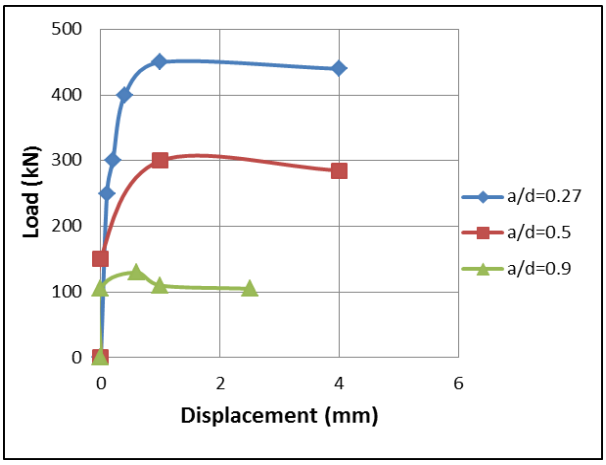

Figure 14. Load-deflection curve for 0.27, 0.5 and 0.9 a/d ratio

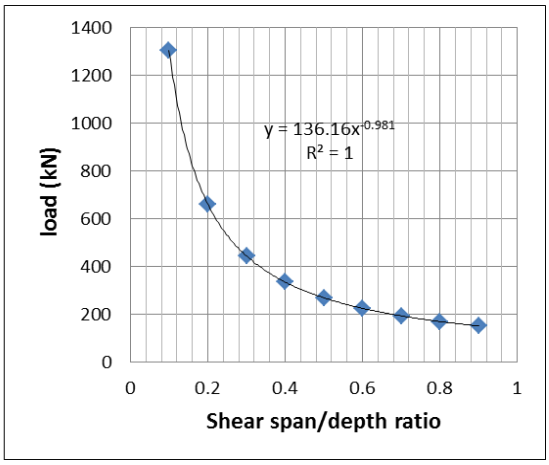

Figure 15. Influence function of shear span depth ratio on shear capacity Of UHPC corbel

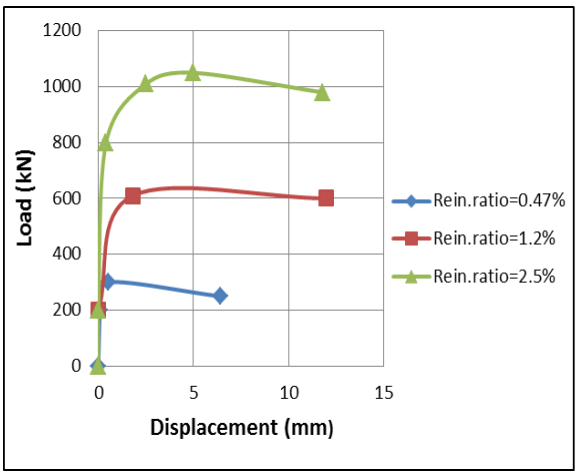

Figure 16. load-deflection curves for ρ=0.47%, 1.2% and 2.5%.

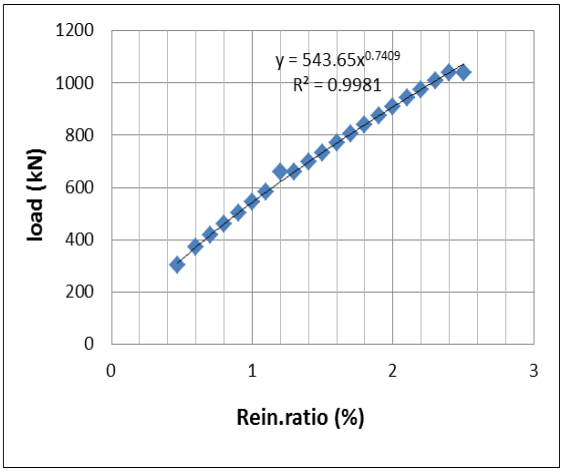

Figure 17. Influence function of reinforcement ratio on shear capacity of UHPC corbels

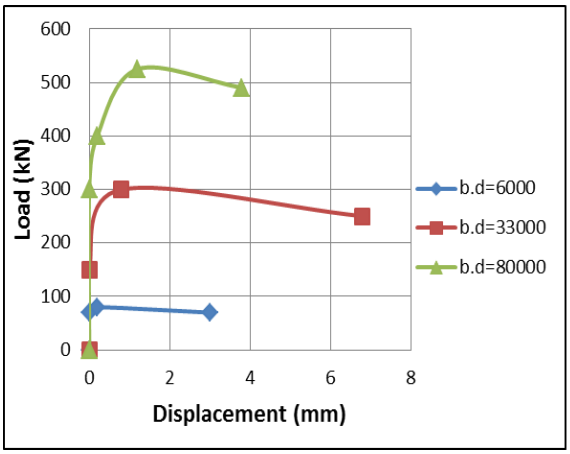

Figure 18. The load-deflection curve for b.d=6000, 33000 and 80000 mm^2

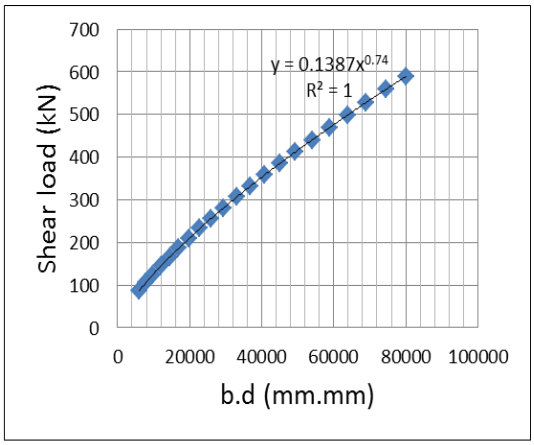

Figure 19. Influence function of the factor b.d on the shear capacity of UHPC corbel

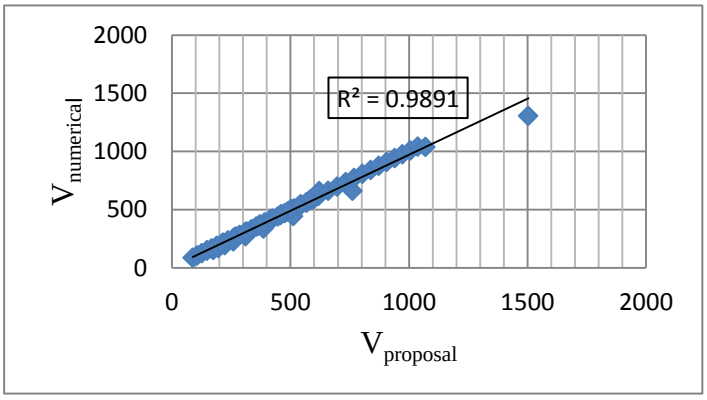

Figure 20. Numerical and calculated corbel shear strength